



Published in final edited form as:

Nat Chem Biol. ; 7(8): 560–565. doi:10.1038/nchembio.594.

## An iron-dependent and transferrin-mediated cellular uptake pathway for plutonium

Mark P. Jensen<sup>1,\*</sup>, Drew Gorman-Lewis<sup>1,2</sup>, Baikuntha Aryal<sup>1,3</sup>, Tatjana Paunesku<sup>4</sup>, Stefan Vogt<sup>5</sup>, Paul G. Rickert<sup>1</sup>, Soenke Seifert<sup>5</sup>, Barry Lai<sup>5</sup>, Gayle E. Woloschak<sup>4</sup>, and L. Soderholm<sup>1</sup>

<sup>1</sup>Chemical Sciences and Engineering Division, Argonne National Laboratory, Argonne, IL 60439 USA

<sup>3</sup>Department of Chemistry, University of Chicago, Chicago, IL 60637 USA

<sup>4</sup>Departments of Radiation Oncology and Radiology, Feinburg School of Medicine, Northwestern University, Chicago, IL 60611, USA

<sup>5</sup>X-ray Science Division, Advanced Photon Source, Argonne National Laboratory, Argonne, IL 60439 USA

### Abstract

Plutonium is a toxic synthetic element with no natural biological function, but it is strongly retained by humans when ingested. Using small angle X-ray scattering, receptor binding assays, and synchrotron X-ray fluorescence microscopy we find that rat adrenal gland (PC12) cells can acquire plutonium *in vitro* through the major iron acquisition pathway, receptor-mediated endocytosis of the iron transport protein serum transferrin; however only one form of the plutonium-transferrin complex is active. Low-resolution solution models of plutonium-loaded transferrins derived from small angle scattering demonstrate that only transferrin with plutonium bound in the protein's C-terminal lobe and iron bound in the N-lobe ( $\text{Pu}_\text{C}\text{Fe}_\text{N}\text{Tf}$ ) adopts the proper conformation for recognition by the transferrin receptor protein. Although the metal binding site in each lobe contains the same donors in the same configuration and both lobes are similar, the differences between transferrin's two lobes act to restrict, but not eliminate, cellular Pu uptake.

Organisms have no natural mechanism for specifically recognizing plutonium (Pu) as it is a non-essential element that until 1941 only existed on earth in biologically insignificant concentrations for at least the last two billion years. Nevertheless, Pu is radiotoxic and is strongly retained by organisms<sup>1</sup>, Pu uptake from an accident, environmental contamination, or a nuclear or radiological attack can pose significant health risks. Plutonium localizes principally in the liver and skeleton in humans where it remains for decades<sup>2</sup>. It associates *in vivo* with the iron-containing proteins serum transferrin and ferritin<sup>3,4</sup>, but despite the danger of plutonium poisoning, the specific molecular-level pathways Pu travels to enter and localize in cells have never been identified<sup>2,5</sup> and no complete structure of a plutonium-

\*To whom correspondence should be addressed. mjensen@anl.gov.

<sup>2</sup>Current address, Department of Earth and Space Sciences, University of Washington, Seattle, WA 98195 USA

#### AUTHOR CONTRIBUTIONS

M.P.J., D.G.-L., and B.P.A. carried out the experiments and analyzed the data. T.P., P.G.R and G.E.W. participated in the cell uptake experiments. T.P., L.S., G.E.W., S.V. and B.L. took part in the SXFM experiments and S.S. assisted with the SAXS measurements. S.S. and S.V. also worked on data reduction and analysis. M.P.J. designed the experiments. M.P.J., D.G.-L., B.P.A., and L.S. wrote the manuscript with input from all the authors.

#### COMPETING FINANCIAL INTERESTS

The authors declare no competing financial interests.

protein complex has ever been reported. Understanding how a synthetic element like plutonium subverts existing biological metal-acquisition pathways to enter cells and where the pathways of plutonium and essential metals, such as iron, converge or diverge could provide important insights into the molecular mechanisms organisms use to distinguish between metal ions and enable new treatments for plutonium poisoning.

Plutonium's chemistry bears limited resemblance to that of biologically important transition metals. Plutonium is highly redox active with four oxidation states (III, IV, V, and VI) potentially relevant to living organisms, although Pu(IV) has long been considered the most important under physiological conditions<sup>6</sup>. Regardless of oxidation state, Pu ions are hard Lewis acids that generally form kinetically labile bonds with ligands<sup>7</sup>. They are also large ions (crystallographic radii = 0.85 – 1.14 Å for CN = 6<sup>8</sup>, depending on the oxidation state) that prefer high coordination numbers; plutonium complexes with coordination numbers of 8 or 9 are common<sup>9</sup>.

While these properties set Pu apart from transition metals commonly encountered in the metallome, Pu and transition metals do share important similarities. Similar to high-valent transition metals, tetravalent Pu is strongly hydrolyzed at physiological pH<sup>10</sup>. In the absence of steric constraints, Pu<sup>4+</sup> tends to form complexes that are about as stable as those of trivalent first row transition metals, notably Fe<sup>3+</sup>, because the metals' charge to radius ratios are similar<sup>1,11</sup>. These properties give plutonium a chemistry that partly resembles transition metals, especially iron. The chemical similarities of Fe and Pu are particularly important to the metal transport protein serum transferrin (Tf). Transferrin functions to strongly bind and carry two Fe<sup>3+</sup> ions into cells, but it also binds Pu<sup>4+</sup> strongly<sup>12</sup> with a reported conditional  $pK_d = 21.25 \pm 0.75$ <sup>13</sup>, and it accounts for 70–90 % of the Pu in serum<sup>3,13</sup>.

Diferric transferrin (holo-transferrin, Fe<sub>2</sub>Tf) delivers iron to mammalian cells through receptor-mediated endocytosis in a multi-step process. Transferrin is a bilobal glycoprotein. Each lobe of Tf, the C-lobe and N-lobe, is composed of two domains with one iron binding site located at the bottom of the inter-domain cleft in each lobe. When an appropriate metal ion and a synergistic anion (i.e., CO<sub>3</sub><sup>2-</sup>) are both present in one binding site, the domains close around the binding site, sequestering the metal and binding it tightly ( $K_d = 10^{-21.4}$  M for Fe<sup>3+</sup>)<sup>14</sup>. When both lobes of Tf are thus properly closed, the metal-transferrin complex is in the proper conformation to be recognized by the transferrin receptor protein (TR) on the cellular surface. At the extracellular pH of 7.4, TR binds Fe<sub>2</sub>Tf strongly ( $K_d = 5$  nM)<sup>15</sup>. Other forms of transferrin, metal-free apo-transferrin and the monoferric transferrins Fe<sub>N</sub>Tf and Fe<sub>C</sub>Tf (with the metal-containing lobe indicated by the subscript N or C), are not in the proper conformation to be well-recognized by TR because one or both of the lobes remain open in the absence of a metal cation<sup>16</sup>. As a result, the receptor binding constants of apo-Tf, Fe<sub>N</sub>Tf, and Fe<sub>C</sub>Tf are at least an order of magnitude smaller than that of Fe<sub>2</sub>Tf-TR<sup>15</sup>.

While some have suggested that transferrin may carry Pu into cells<sup>17</sup>, extensive *in vitro* experiments have been taken to imply that plutonium-transferrin complexes are not taken into cells in a manner similar to the iron-transferrin complex<sup>2,18–20</sup>, presumably because Pu<sup>4+</sup> is a larger ion than Fe<sup>3+</sup> and strongly prefers higher coordination numbers. Instead, an ill-defined uptake pathway, which does not involve transferrin, has been invoked as the source of intracellular Pu<sup>18,20</sup>.

Studying the conformations and biochemical interactions of plutonium-transferrin complexes using a low specific activity plutonium isotope (<sup>242</sup>Pu) to minimize radiation effects, we found that mammalian cells could acquire Pu through the common Fe uptake pathway of receptor-mediated endocytosis of metallo-transferrins. However, to be taken into the cell by receptor-mediated endocytosis, Pu needed help from Fe because only one isomer

of the monoplutonium-monoiron-transferrin complex was active. In the active form of the plutonium-laden protein, Pu<sup>4+</sup> was bound in the metal binding site of the protein's C-terminal lobe and Fe<sup>3+</sup> was bound in the protein's N-lobe (Pu<sub>C</sub>Fe<sub>N</sub>Tf). All other forms of plutonium-transferrin that could exist *in vivo* failed to adopt the proper conformation for receptor recognition and uptake. Although the metal binding site in each lobe contains the same donors in the same configuration and both lobes are similar<sup>14,21</sup>, the differences between transferrin's two lobes restricted, but did not eliminate, cellular Pu uptake.

## RESULTS

### Receptor binding of plutonium-transferrins

To understand how cells take up plutonium and if the cellular uptake mechanisms of Fe<sup>3+</sup> and Pu<sup>4+</sup> diverge, we systematically examined the binding of Pu-Tf complexes to the transferrin receptor protein, which is a prerequisite for cellular uptake of a metallo-transferrin. Receptor binding assays of plutonium-bearing human transferrins were conducted using the soluble extracellular fragment of human transferrin receptor 1 isolated from serum<sup>22</sup>, which retains its capacity to bind Fe<sub>2</sub>Tf<sup>23</sup>. The binding of the controls apo-Tf and Fe<sub>2</sub>Tf (Fig. 1) were as expected from the previously reported binding constants<sup>15,24</sup>. The two Fe<sup>3+</sup> cations in diferric transferrin were then systematically replaced with Pu<sup>4+</sup>, individually producing the mixed monoplutonium-monoiron-transferrin complexes Pu<sub>C</sub>Fe<sub>N</sub>Tf and Fe<sub>C</sub>Pu<sub>N</sub>Tf, and the diplutonium-transferrin complex Pu<sub>2</sub>Tf (i.e., Pu<sub>C</sub>Pu<sub>N</sub>Tf), which were incubated with the transferrin receptor. The receptor binding assays of the three plutonium-transferrins (Fig. 1) indicated that each of these metallo-transferrins could bind soluble TR under our experimental conditions. However, the different forms of Pu-Tf showed different receptor binding behaviors. The affinity of TR for Pu<sub>2</sub>Tf and Fe<sub>C</sub>Pu<sub>N</sub>Tf, was substantially lower than for Pu<sub>C</sub>Fe<sub>N</sub>Tf and Fe<sub>2</sub>Tf, suggesting that although Pu<sup>4+</sup> binds to Tf in the Fe<sup>3+</sup> binding site<sup>13</sup>, neither Pu<sub>2</sub>Tf nor Fe<sub>C</sub>Pu<sub>N</sub>Tf would be recognized at physiological concentrations. In contrast, Pu<sub>C</sub>Fe<sub>N</sub>Tf should be recognized by TR.

### Solution conformations of plutonium-transferrins

One form of plutonium-transferrin, Pu<sub>C</sub>Fe<sub>N</sub>Tf, bound the transferrin receptor well but the two other forms, Fe<sub>C</sub>Pu<sub>N</sub>Tf and Pu<sub>2</sub>Tf, did not. Because the transferrin receptor only binds transferrin well if both the protein's lobes are in the closed conformation, we examined a series of metallo-transferrins using small-angle X-ray scattering (SAXS) to obtain low resolution solution models of the bovine proteins. The scattering profiles of the transferrins (see Supplementary Results and Supplementary Fig. S1a online) fell into three distinct groups. Based on the scattering of the natural transferrins, we assigned these groups of scattering curves to transferrin with both lobes open, one lobe open and one lobe closed, or both lobes closed, which we term open, mixed, and closed transferrins, respectively. The scattering profiles of the closed transferrins (i.e., Fe<sub>2</sub>Tf, Pu<sub>C</sub>Fe<sub>N</sub>Tf, and In<sub>2</sub>Tf, di-indium transferrin) were qualitatively distinguished from the other curves by a distinct drop in scattering intensity between 0.15 and 0.20 Å<sup>-1</sup> (Supplementary Fig. S1b)<sup>25</sup>.

The differences between the protein conformations indicated by the scattering were clarified by *ab initio* shape reconstruction of low-resolution protein models from the SAXS by simulated annealing of dummy atom (bead) models<sup>26</sup>. The resulting three-dimensional solution structures of the proteins calculated from the scattering data agree well with the reported crystal structures of serum transferrin<sup>27,28</sup> (Fig. 2a and Supplementary Fig. S2). As depicted in Figure 2, the two lobes of each metallo-transferrin are clearly visible at the top and bottom of each model, as was the open or closed conformation of each lobe. Most importantly, the structures of Pu<sub>C</sub>Fe<sub>N</sub>Tf and closed Fe<sub>2</sub>Tf, which both bound TR well, were very similar (Figs. 2a and 2b), and both had two closed lobes. In contrast, the conformations

of the other plutonium-bearing transferrins,  $\text{Fe}_\text{C}\text{Pu}_\text{N}\text{Tf}$  and  $\text{Pu}_2\text{Tf}$ , were clearly mixed. Those models (Figs. 2a and 2b) showed one smaller closed lobe at the bottom of the displayed structural model and one open lobe at the top with a cleft between the lobe's two domains, just as observed for mixed  $\text{Fe}_\text{C}\text{Tf}$ .

Although the resolution of these measurements did not allow direct identification of the C- and N-lobes of each metallo-transferrin from the SAXS data, the systematic substitution of  $\text{Pu}^{4+}$  into Tf allowed identification of the one open lobe observed for  $\text{Fe}_\text{C}\text{Pu}_\text{N}\text{Tf}$  and  $\text{Pu}_2\text{Tf}$ .  $\text{Fe}^{3+}$  binding causes lobe closure under the conditions of our experiments. Consequently, the iron-containing C-lobe of  $\text{Fe}_\text{C}\text{Pu}_\text{N}\text{Tf}$  was closed and the plutonium-containing N-lobe must be the open lobe observed for this form of the protein. This implied that the N-lobe of  $\text{Pu}_2\text{Tf}$  also was open. In fact, the conformation and overall dimensions of the open lobe determined for the mixed transferrins ( $\text{Fe}_\text{C}\text{Tf}$ ,  $\text{Fe}_\text{C}\text{Pu}_\text{N}\text{Tf}$ , and  $\text{Pu}_2\text{Tf}$ ) from the SAXS data matched the crystal structure of the open N-terminal half apo-transferrin fragment<sup>29</sup> well, as depicted for  $\text{Pu}_2\text{Tf}$  in Fig. 2a.

The conformation of  $\text{Pu}_2\text{Tf}$  indicated that transferrin's two iron-binding sites respond to  $\text{Pu}^{4+}$  differently. The N-lobe of  $\text{Pu}_2\text{Tf}$  was open; therefore the second plutonium cation in the C-lobe must promote C-lobe closure because the SAXS data indicated that one lobe of  $\text{Pu}_2\text{Tf}$  was closed (Fig. 2a). Since  $\text{Pu}^{4+}$  in the C-lobe and  $\text{Fe}^{3+}$  in either lobe caused lobe closure, both lobes of  $\text{Pu}_\text{C}\text{Fe}_\text{N}\text{Tf}$  were expected to be closed. The structural reconstruction of  $\text{Pu}_\text{C}\text{Fe}_\text{N}\text{Tf}$  confirmed this (Figs. 2a and 2b). Although  $\text{Pu}_2\text{Tf}$  and  $\text{Fe}_\text{C}\text{Pu}_\text{N}\text{Tf}$  adopted the mixed conformation with one open and one closed lobe, solutions of  $\text{Pu}_\text{C}\text{Fe}_\text{N}\text{Tf}$  contained the protein in a fully closed configuration that matched the native form of the protein found for  $\text{Fe}_2\text{Tf}$ . The slight deviations observed between the structures of  $\text{Fe}_2\text{Tf}$  and  $\text{Pu}_\text{C}\text{Fe}_\text{N}\text{Tf}$  (Fig. 2c) were within the uncertainty of the experiment and analysis, and principally arose from the slightly different maximum protein diameters derived from the SAXS data used for the shape reconstruction ( $D_{\text{max}} = 104 \pm 10 \text{ \AA}$  for  $\text{Pu}_\text{C}\text{Fe}_\text{N}\text{Tf}$  vs.  $100 \pm 10 \text{ \AA}$  for  $\text{Fe}_2\text{Tf}$ , see Supplementary Table S1).

### Cellular uptake of plutonium-transferrins

Plutonium's inability to induce closure of transferrin's N-lobe explained the receptor binding experiments and implied that under physiological conditions only  $\text{Pu}_\text{C}\text{Fe}_\text{N}\text{Tf}$ , the sole closed plutonium-transferrin complex, could be recognized by TR and incorporated into cells through receptor-mediated endocytosis. To test this hypothesis, we incubated PC12 cells for 3 hours in complete growth medium supplemented with rat transferrin presented as either closed  $\text{Pu}_\text{C}\text{Fe}_\text{N}\text{Tf}$ , which should be recognized and carry Pu into cells, or mixed  $\text{Fe}_\text{C}\text{Pu}_\text{N}\text{Tf}$ , which should not. The elemental content and distribution in individual cells was monitored with synchrotron X-ray fluorescence microscopy (SXF) (Fig. 3a–e, Supplementary Figs. S3 and S4, and Supplementary Table S2). As expected from the protein conformations and receptor binding experiments, Pu presented as closed  $\text{Pu}_\text{C}\text{Fe}_\text{N}\text{Tf}$  was taken into the cells (Figs. 3b and 3e), and localized in the cytoplasm (Supplementary Figs. S3d–f). The average intracellular content of the Pu containing cells was  $1.6 \pm 0.3 \text{ ng Pu/cm}^2$  ( $\pm$ S.E.M at 95% confidence,  $n = 8$ ). In contrast, the average cellular uptake of Pu from mixed  $\text{Fe}_\text{C}\text{Pu}_\text{N}\text{Tf}$  was sharply reduced to only  $0.3 \pm 0.2 \text{ ng Pu/cm}^2$  ( $\pm$ S.E.M at 95% confidence,  $n = 21$ ), as illustrated in Figures 3c and 3e.

To ensure that the cells remained viable over the course of treatment at the concentrations of  $^{242}\text{Pu}$  used, cell viability was quantified by trypan blue exclusion in separate experiments prior to the SXFM measurements. Individual determinations of the viability of cells grown in media supplemented with the highest concentrations of Pu, chloroquine (*vide infra*), or Pu and chloroquine ranged from 86 to 105% of control cells with a run to run range of  $\pm 10\%$  for each measurement of control or treated cells. The average cell viabilities (Supplementary

Table S3) were indistinguishable from those of PC12 control samples for the first 3 hours of incubation.

The initial plutonium-transferrin uptake experiments were consistent with receptor-mediated endocytosis of  $\text{Pu}_\text{C}\text{Fe}_\text{N}\text{Tf}$ , just like  $\text{Fe}_2\text{Tf}$ . To further explore this possibility, the cellular uptake of Pu from closed  $\text{Pu}_\text{C}\text{Fe}_\text{N}\text{Tf}$  was studied under conditions that would reduce Pu uptake by that pathway. First, Pu uptake from complete media supplemented with an equimolar mixture of  $\text{Pu}_\text{C}\text{Fe}_\text{N}\text{Tf}$  and  $\text{Fe}_2\text{Tf}$  was examined. While PC12 cells still took in Pu from this medium, the average intracellular concentration of Pu (Fig. 3e) decreased to  $39 \pm 15\%$  of the value observed for cells incubated with  $\text{Pu}_\text{C}\text{Fe}_\text{N}\text{Tf}$  alone (error propagated  $\pm$ S.E.M., 4  $\text{Fe}_2\text{Tf}$  co-treated cells studied). This was in reasonable agreement with the value expected for simple competition between equal concentrations of  $\text{Pu}_\text{C}\text{Fe}_\text{N}\text{Tf}$  and  $\text{Fe}_2\text{Tf}$  (50%) if the all aspects of the uptake and retention of Pu and Fe are equivalent and the presence of  $12.5 \mu\text{M}$   $\text{Fe}_2\text{Tf}$  does not down regulate transferrin-mediated uptake over the time frame of our experiment.

Transferrin endocytosis also is temperature dependent<sup>30</sup>. No difference was discernable between the uptake of  $\text{Pu}_\text{C}\text{Fe}_\text{N}\text{Tf}$  at  $25^\circ\text{C}$  ( $1.5 \pm 0.5 \text{ ng Pu/cm}^2$ ,  $\pm$ S.E.M. at 95% confidence,  $n = 3$  cells) and  $37^\circ\text{C}$  ( $1.8 \pm 0.4 \text{ ng Pu/cm}^2$ ,  $\pm$ S.E.M. at 95% confidence,  $n = 5$  cells), presumably because of normal cell-to-cell variations in the elemental content and the small sample size. However, lowering the incubation temperature to  $4^\circ\text{C}$  curtailed Pu uptake as expected for active uptake of  $\text{Pu}_\text{C}\text{Fe}_\text{N}\text{Tf}$  by endocytosis. Bulk Pu uptake at  $4^\circ\text{C}$  was  $17 \pm 17\%$  of the uptake of cells incubated at  $37^\circ\text{C}$  ( $n = 3$ , error propagated  $\pm$ S.E.M. at 95% confidence).

To further study Pu uptake from closed  $\text{Pu}_\text{C}\text{Fe}_\text{N}\text{Tf}$ , PC12 cells also were incubated for 3 hours in complete media supplemented with rat  $\text{Pu}_\text{C}\text{Fe}_\text{N}\text{Tf}$  ( $12.5 - 25 \mu\text{M}$ ) and chloroquine ( $50 \mu\text{M}$ ), which is known to disrupt the uptake of iron through receptor-mediated endocytosis of  $\text{Fe}_2\text{Tf}$ . It does so by preventing complete acidification of the endosomes thereby inhibiting iron release from the  $\text{Fe}_2\text{Tf-TR}$  complex into the endosomes<sup>30</sup>. In these experiments, chloroquine treatment severely reduced Pu uptake from  $\text{Pu}_\text{C}\text{Fe}_\text{N}\text{Tf}$  by intact cells (Fig. 3e) to an average of  $0.2 \pm 0.3 \text{ ng Pu/cm}^2$  ( $\pm$ S.E.M. at 95% confidence, 8 cells studied). While very little Pu was associated with intact chloroquine-treated cells, measurable Pu was found in the SXFM maps associated with cellular debris (Fig. 3d) in the chloroquine treated system. This implied that chloroquine inhibited Pu uptake by living cells, but it did not inhibit Pu binding to the intracellular constituents from ruptured cells. Thus, a drug that disrupts Fe release from  $\text{Fe}_2\text{Tf}$  into the endosomes also disrupted the active uptake of Pu from  $\text{Pu}_\text{C}\text{Fe}_\text{N}\text{Tf}$  by living cells.

The lack of plutonium uptake from mixed  $\text{Fe}_\text{C}\text{Pu}_\text{N}\text{Tf}$ , coupled with the proportional reduction in Pu uptake from mixtures of  $\text{Fe}_2\text{Tf}$  and  $\text{Pu}_\text{C}\text{Fe}_\text{N}\text{Tf}$  and the ability of low temperatures or the presence of chloroquine to inhibit plutonium uptake from closed  $\text{Pu}_\text{C}\text{Fe}_\text{N}\text{Tf}$  demonstrated that  $\text{Pu}_\text{C}\text{Fe}_\text{N}\text{Tf}$ , which has the same closed conformation as  $\text{Fe}_2\text{Tf}$ , followed  $\text{Fe}_2\text{Tf}$  into the cells through receptor-mediated endocytosis and was not taken up through non-specific pinocytosis.

## DISCUSSION

Our studies each indicated that plutonium could infiltrate mammalian cells using the normal Tf-TR iron uptake system, but only with help from iron and only for one particular isomer of the plutonium-iron-transferrin complex,  $\text{Pu}_\text{C}\text{Fe}_\text{N}\text{Tf}$ . Earlier attempts to trace the cellular uptake of plutonium either used  $\text{Pu}_2\text{Tf}$ ,  $\text{PuTf}$ , or made no attempt to control the metal population of transferrin, producing conflicting results that discredited transferrin-mediated

cellular uptake of plutonium without clearly defining another specific uptake pathway<sup>2,18–20</sup>. Other pathways for plutonium uptake that do not involve transferrin likely exist, as is known for iron<sup>31</sup>, but our results demonstrated that Pu<sub>C</sub>Fe<sub>N</sub>Tf was capable of efficiently delivering Pu to mammalian cells *in vitro* through receptor-mediated endocytosis.

The specific requirement for iron binding in the N-lobe of transferrin restricted plutonium's ability to exploit the transferrin-mediated uptake pathway; however Pu<sub>C</sub>Fe<sub>N</sub>Tf likely would constitute a substantial portion of the Pu-Tf species in the blood of exposed individuals. In circulating human blood transferrin concentrations normally range between 25 and 46 μM<sup>32</sup>. Iron usually consumes only a fraction of transferrin's iron-binding capacity, leaving ample capacity for transferrin to bind plutonium and giving rise to a distribution of different transferrin species. For normal blood iron loadings, an average distribution of transferrin species of 37% apo-Tf, 45% Fe<sub>N</sub>Tf, 8% Fe<sub>C</sub>Tf, and 11% Fe<sub>2</sub>Tf in human serum has been reported<sup>33</sup>. The precursors to Pu<sub>C</sub>Fe<sub>N</sub>Tf, Fe<sub>N</sub>Tf and apo-Tf (which can react to form Pu<sub>C</sub>Tf), constitute the major fraction of the transferrin in human serum. Thus the inability of plutonium to trigger N-lobe closure in serum transferrin is not sufficient to prohibit Pu uptake through the Tf-TR pathway *in vivo* where iron is available to fill the N-lobe.

Several possible advantages of modern bilobal transferrins over their single-lobed progenitors have been proposed. As a partial iron mimic, the interactions between plutonium and transferrin suggest another, enhanced selectivity for iron. By itself, transferrin does not effectively discriminate against the man-made element plutonium, binding Pu<sup>4+</sup> almost as strongly as Fe<sup>3+</sup><sup>13</sup>, but the bilobal nature of transferrin and the differences between the lobes confer a measure of selectivity against plutonium to the Tf-TR uptake system. Contrary to predictions<sup>34,35</sup>, Pu<sup>4+</sup> and Fe<sup>3+</sup> are sufficiently different that plutonium binding did not trigger closure of the N-lobe. Therefore, neither Pu<sub>2</sub>Tf nor Fe<sub>C</sub>Pu<sub>N</sub>Tf were efficiently recognized by the transferrin receptor, and cellular uptake of Pu was diminished. Plutonium could overcome the selectivity of the multi-step metal recognition system of the Tf-TR pair only with the assistance of Fe through the formation of Pu<sub>C</sub>Fe<sub>N</sub>Tf, which efficiently bound TR.

The Tf-TR iron uptake system achieves its partial selectivity for iron over plutonium in spite of the similarity of the C- and N-lobes, which show high sequence similarity (40–50% for serum transferrins)<sup>36</sup>. The residues involved in metal binding are completely conserved between the two lobes and also are conserved in the closely related proteins lactoferrin (Lf) and ovotransferrin<sup>14</sup>. Since the identity and the configuration of the binding residues are the same in both lobes of serum transferrin, the partial discrimination of the Tf-TR system against Pu could not arise from plutonium's presumed direct interactions with the binding residues (2 Tyr, 1 Asp, 1 His) in the metal binding sites. Moreover, when lactoferrin binds Ce<sup>4+</sup>, another tetravalent f-element cation with the same size and coordination preferences as Pu<sup>4+</sup>, the crystal structure of dimeric lactoferrin (Ce<sub>2</sub>Lf) shows that the coordination environment of Ce<sup>4+</sup> matches that of Fe<sup>3+</sup> in Fe<sub>2</sub>Lf and that both the C-lobe and the N-lobe are closed<sup>35</sup>. Consequently, the different responses of transferrin's two lobes to Pu binding and the ability of the Tf-TR uptake system's ability to attenuate Pu uptake appear to arise from one or more known structural differences between the lobes<sup>28,37</sup> outside of the actual metal binding sites.

The protein conformations we observed for the plutonium-iron-transferrin complexes also suggest that mixed-metal transferrin complexes may play an important role in the metallome by allowing an unsuspected trafficking pathway for naturally occurring metals. Transferrin is known to bind over 30 different metals, but the cellular uptake of the metal-transferrin complexes is believed relevant for only a few of them<sup>14</sup>. Since transferrin's two lobes can react differently to binding the same metal ion, the uptake of mixed iron-metal-transferrin

complexes ( $M_CFe_NTf$  or  $Fe_CM_NTf$ ) *in vivo* may represent substantial uptake pathways for other metals as well if metal binding induces closure of one lobe but not the other. The relevance of mixed-metal transferrins would not be apparent from studies of the receptor-binding or cellular uptake of simple  $M_2Tf$  complexes as one lobe of  $M_2Tf$  would be open and the complex would not be recognized by TR.

The intracellular pathways plutonium follows between its putative release from Tf in the endosomes and its retention in the cytoplasm have yet to be identified, but our demonstration that a specific form of plutonium-transferrin entered mammalian cells using the normal  $Fe_2Tf$ -TR pathway is of practical significance because this well-defined pathway presents multiple targets to block plutonium uptake and spare cells from its highly destructive  $\alpha$ -radiation. Currently approved therapies for plutonium poisoning, based on ligands that strongly bind Pu, are unable to extract all intracellular Pu<sup>1,38,39</sup>. In contrast, novel strategies to disrupt the  $Pu_CFe_NTf$ -TR pathway could preempt plutonium accumulation in cells. Such strategies might include blocking the binding of  $Pu_CFe_NTf$  to TR, or inhibiting the intracellular release of Pu in the endosome (mimicking the action of chloroquine in our experiments), which would keep Pu from accumulating in cells and could promote faster clearance from the body, particularly if used in conjunction with plutonium-specific chelators.

## METHODS

### Protein Preparation

Bovine, human, and rat serum transferrins ( $\geq 98\%$ ) were obtained from commercial sources (Sigma-Aldrich or Rockland Immunochemical), and further purified by gel chromatography on superfine Sephadex G-100 (GE Healthcare). Protein concentrations were measured by BCA protein assay or UV spectroscopy<sup>40</sup>. Metal concentrations were measured by UV-visible spectroscopy for Fe or liquid scintillation counting (LSC) of <sup>242</sup>Pu. Iron saturation of transferrin was ensured by adding freshly prepared pH 4 solutions of  $Fe(NTA)_2^{3-}$  ( $NTA^{3-}$  = nitrilotriacetate) to transferrin in 0.1 M NaCl/0.01 M HEPES/0.005 M  $NaHCO_3$ , while iron depletion was achieved by exposing the protein to 0.1 M sodium citrate/0.1 M acetate buffer solutions at pH 4.5. Unreacted material was removed by repeated buffer exchange with ultracentrifugation through a 30 kDa Centricon filter (Millipore). Monoferric transferrins  $Fe_CTf$  and  $Fe_NTf$  were prepared according to literature methods.<sup>40,41</sup> The purity of the preparations was established by urea-PAGE (see Supplementary Methods and Fig. S5 online). <sup>242</sup>Pu-loaded transferrins were prepared by mixing solutions of Pu-citrate or Pu-NTA complexes with the appropriate transferrin in 0.1 M NaCl/0.01 M HEPES/0.005 M  $NaHCO_3$  at pH 7.4 (Supplementary Methods and accompanying Supplementary Figures S6 and S7).

### Receptor Binding

Soluble human transferrin receptor ( $\geq 95\%$ , Hystest) consisting of extracellular residues 101–760 of the intact receptor was used as received. Solutions containing a 1:1 ratio of TR and Pu-loaded human serum transferrin as  $Pu_2Tf$ ,  $Pu_CFe_NTf$ , or  $Fe_CPu_NTf$  at 1  $\mu M$  were allowed to react for at least 15 minutes at 23 °C before isolation of the receptor-bound transferrin using gel chromatography on superfine Sephadex G-100<sup>42</sup>. Protein was quantified by UV-visible spectroscopy. Plutonium was quantified by LSC.

### Small-angle X-ray Scattering

SAXS measurements at Advanced Photon Source beamline 12-ID-B<sup>43</sup> used bovine transferrin solutions of 5, 10, and 20 mg/mL purified by gel chromatography to separate protein oligomers. A quartz capillary cell<sup>44</sup> was used for non-radioactive samples.

Plutonium-containing samples were measured in cells with polychlorotrifluoroethylene and Kapton (Chemplex) windows<sup>45</sup>. Scattering was measured at 18.0 and 20.0 keV with a 2048 × 2048 pixel MAR-CCD-165 detector 2 m from the sample. The scattering vector,  $Q = 4\pi(\sin \theta)/\lambda$  where  $2\theta$  is the scattering angle and  $\lambda$  is the X-ray wavelength, was calibrated against a silver behenate standard at each energy. The usable  $Q$  range of the circularly averaged data was limited to  $0.018 < Q < 0.30 \text{ \AA}^{-1}$  by background scattering from the windows required to encapsulate the radioactive samples. Except for Pu<sub>C</sub>Fe<sub>N</sub>Tf, the samples were stable to radiation damage for more than 5 seconds and the scattering was taken as the average of five 1 second exposures. Pu<sub>C</sub>Fe<sub>N</sub>Tf was measured in a separate campaign with a tightly focused X-ray beam. Under these conditions, the sample was radiation stable for 0.5 seconds. The scattering of the Pu<sub>C</sub>Fe<sub>N</sub>Tf samples was determined from single 0.5 second exposures on replicate samples. The scattering data was analyzed using the ATSAS program suite<sup>46</sup> to produce most probable structural models for each protein (Supplementary Methods and Supplementary Fig. S8).

### Cell Uptake and SXFM Imaging

PC12 cells (ATCC) were grown in F12K medium supplemented with 12.5 % horse serum, 2.5% fetal calf serum, and antibiotics in humidified 5% CO<sub>2</sub> at 37°C. Cells were plated in the appropriate density (ca. 70% confluency) the day before Pu exposure. The cells were then serum-starved overnight and used without other pre-treatment. Cells were exposed to 12.5 – 50 μM of the different forms of Pu-containing rat transferrin for 3 hours at 4, 25 or 37 °C in complete F12K medium with serum. Diferric rat transferrin (12.5 μM) or chloroquine diphosphate (50 μM) was also added to the media for the full incubation time in studies of the inhibition of Pu uptake. Cell viability was checked by trypan blue exclusion in select cases, and was typically 80–90%, showing no difference from Pu-free control cells (Supplementary Table S3). Surface-sorbed Pu was removed by washing the cells with the extracellular chelating agent EGTA (0.01 M) in 0.1 M NaCl thrice. The efficacy of this procedure for removing surface-bound Pu-transferrins was checked by a 20 minute post-washing incubation with 0.2% pronase at 4 °C<sup>30</sup>. The amount of cell-associated Pu for the pronase treated cells, quantified by LSC, was  $81 \pm 22\%$  that of the control cells ( $n = 3$ , error propagated ±S.E.M. at 95% confidence).

After washing, cells were liberated from the culture bottles by scraping into 0.1 M NaCl/0.01 M EGTA, and pelleted by centrifugation. The cells were then deposited on polyvinyl formal-coated copper electron microscopy grids from fresh NaCl/EGTA solutions and air dried without chemical fixation of the cells. The grids were mounted, encapsulated between two 500 nm silicon nitride windows, and sealed beneath a layer of 6 μm polypropylene or 8 μm Kapton film. Optical micrographs of the cells were obtained with a Leica DMRXE microscope at 10×, 20×, or 40× using QCapture software (QImaging) and were used without alteration.

Cellular distributions of the elements from P though Pu were measured simultaneously by SXFM in a He atmosphere on the Advanced Photon Source 2-ID-D hard X-ray microprobe beamline<sup>47</sup>. The 18.1 keV X-ray beam was focused to a 0.2 μm × 0.5 μm or smaller spot and maps of the cells were obtained by raster scanning the samples in 0.5 μm steps. The monochromator energy was calibrated by setting the first inflection point of the K-edge of a Zr foil to 17.998 keV.

The fluorescence signal for each element at each spatial pixel was converted to elemental content in μg/cm<sup>2</sup> after calibration with elemental standards as previously described<sup>48</sup>. In the absence of a traceable concentration standard, Pu was quantified by extrapolation of the calibration curve obtained from the X-ray fluorescence signals of the multi-element thin film standards NBS-1832 and NBS-1833 (NIST), taking into account relevant differences such as



photo-electric absorption of incident photons, absorption in the Be detector window, and fluorescence yield. The estimated absolute accuracy is better than 40%, and the relative accuracy is better than 10%. The resulting elemental maps were visualized and analyzed using the program MAPS<sup>49</sup>.

## Supplementary Material

Refer to Web version on PubMed Central for supplementary material.

## Acknowledgments

The work at Argonne National Laboratory, including the use of the Advanced Photon Source, was supported by the U. S. Department of Energy, Office of Basic Energy Sciences, under Contract No. DE-AC02-06CH11357, while work at Northwestern University was supported by NIH grants EB002100 and U54CA119341.

## References

1. Gorden AEV, Xu J, Raymond KN, Durbin P. Rational design of sequestering agents for plutonium and other actinides. *Chem Rev.* 2003; 103:4207–4282. [PubMed: 14611263]
2. Durbin, PW. Actinides in animals and man. In: Morss, LR.; Edelman, NM.; Fuger, J., editors. *The chemistry of the actinide and transactinide elements*. Vol. 5. Springer; Dordrecht: 2006. p. 3339-3440.
3. Boocock G, Popplewell DS. Distribution of plutonium in serum proteins following intravenous injection into rats. *Nature.* 1965; 208:282–283. [PubMed: 5882454]
4. Boocock G, Danpure CJ, Popplewell DS, Taylor DM. The subcellular distribution of plutonium in rat liver. *Radiat Res.* 1970; 42:381–396. [PubMed: 4315168]
5. Duffield, JR.; Taylor, DM. The biochemistry of the actinides. In: Freeman, AJ.; Keller, C., editors. *Handbook on the physics and chemistry of the actinides*. Vol. 4. Elsevier Science; New York: 1986. p. 129-157.
6. Taylor, DM. Chemical and physical properties of plutonium. In: Hodge, HC.; Stannard, JN.; Hursh, JB., editors. *Uranium, plutonium, transplutonic elements*. Vol. 36. Springer-Verlag; New York: 1973. p. 323-347. *Handbook of experimental pharmacology*
7. Choppin GR. Solution chemistry of the actinides. *Radiochim Acta.* 1983; 32:43–53.
8. Shannon RD. Revised effective ionic radii and systematic studies of interatomic distances in halides and chalcogenides. *Acta Cryst.* 1976; A32:751–767.
9. Clark, DL.; Hecker, SS.; Jarvinen, GD.; Neu, MP. Plutonium. In: Morss, LR.; Edelman, NM.; Fuger, J., editors. *The chemistry of the actinide and transactinide elements*. Vol. 2. Springer; Dordrecht: 2006. p. 813-1264.
10. Allard B, Kipatsi H, Liljenzin JO. Expected species of uranium, neptunium and plutonium in neutral aqueous solutions. *J Inorg Nucl Chem.* 1980; 42:1015–1027.
11. Raymond KN, Smith WL. Actinide-specific sequestering agents and decontamination applications. *Struct Bonding.* 1981; 43:159–186.
12. Jeanson A, et al. The role of transferrin in actinide(IV) uptake: Comparison with iron(III). *Chem-Eur J.* 2010; 16:1378–1387. [PubMed: 19950335]
13. Taylor DM. The bioinorganic chemistry of actinides in blood. *J Alloys Compds.* 1998; 271–273:6–10.
14. Sun H, Li H, Sadler PJ. Transferrin as a metal ion mediator. *Chem Rev.* 1999; 99:2817–2842. [PubMed: 11749502]
15. Mason AB, et al. Mutational analysis of C-lobe ligands of human serum transferrin: Insights into the mechanism of iron release. *Biochemistry.* 2005; 44:8013–8021. [PubMed: 15924420]
16. Cheng Y, Zak O, Aisen P, Harrison SC, Walz T. Structure of the human transferrin receptor-transferrin complex. *Cell.* 2004; 116:565–576. [PubMed: 14980223]
17. Hoyes KP, et al. Transferrin-mediated uptake of plutonium by spermatogenic tubules. *Int J Radiat Biol.* 1996; 70:467–471. [PubMed: 8862458]

18. Planas-Bohne F, Rau W. Comparison of the binding of  $^{59}\text{Fe}$ - and  $^{239}\text{Pu}$ -transferrin to rat liver cell membranes. *Human Exp Toxicol.* 1990; 9:17–24.
19. Grossmann JG, et al. Metal-induced conformational changes in transferrins. *J Mol Biol.* 1993; 229:585–590. [PubMed: 8433360]
20. Duffield, JR.; Taylor, DM.; Williams, DR. The biochemistry of the f-elements. In: Gschneidner, KA., Jr; Eyring, L.; Choppin, GR.; Lander, GH., editors. *Handbook on the physics chemistry of the rare earths.* Vol. 18. Elsevier Science; New York: 1994. p. 591-621.
21. Baker, EN. Structure and reactivity of transferrins. In: Sykes, AG., editor. *Advances in inorganic chemistry.* Vol. 41. Academic Press; San Diego: 1994. p. 389-463.
22. Shih YJ, et al. Serum transferrin receptor is a truncated form of tissue receptor. *J Biol Chem.* 1990; 265:19077–19081. [PubMed: 2229063]
23. Giannetti AM, Snow PM, Zak O, Bjorkman PJ. Mechanism for multiple ligand recognition by the human transferrin receptor. *PLoS Biology.* 2003; 1:341–350.
24. Lebrón JA, et al. Crystal structure of the hemochromatosis protein HFE and characterization of its interaction with transferrin receptor. *Cell.* 1998; 93:111–123. [PubMed: 9546397]
25. Grossmann JG, et al. X-ray solution scattering reveals conformational changes upon iron uptake in lactoferrin, serum and ovo-transferrins. *J Mol Biol.* 1992; 225:811–819. [PubMed: 1602483]
26. Svergun DI. Restoring low resolution structure of biological macromolecules from solution scattering using simulated annealing. *Biophys J.* 1999; 76:2879–2886. [PubMed: 10354416]
27. Zuccola, HJ. PhD Dissertation. Georgia Institute of Technology; 1992. The crystal structure of monoferric human serum transferrin.
28. Hall DR, et al. The crystal and molecular structures of diferric porcine and rabbit serum transferrin at resolutions of 2.15 and 2.60 Å, respectively. *Acta Cryst D.* 2002; 58:70–80. [PubMed: 11752780]
29. Jeffrey PD, et al. Ligand-induced conformational change in transferrins: Crystal structure of the open form of the N-terminal half-molecule of human transferrin. *Biochemistry.* 1998; 37:13978–13986. [PubMed: 9760232]
30. Iacopetta BJ, Morgan EH. The kinetics of transferrin endocytosis and iron uptake from transferrin in rabbit reticulocytes. *J Biol Chem.* 1983; 258:9108–9115. [PubMed: 6135697]
31. Wessling-Resnick M. Iron transport. *Annu Rev Nutr.* 2000; 20:129–151. [PubMed: 10940329]
32. Hagler, HK.; Kumar, V.; Robbins, SL. Interactive case study companion to Robbins Pathologic Basis of Disease. 6. W B Saunders Co; 1999.
33. Leibman A, Aisen P. Distribution of iron between the binding sites of transferrin in serum: Methods and results in normal human subjects. *Blood.* 1979; 53:1058–1065. [PubMed: 444649]
34. Harris WR, Carrano CJ, Pecoraro VL, Raymond KN. Siderophilin metal coordination. 1 Complexation of thorium by transferrin: Structure-function implications. *J Am Chem Soc.* 1981; 103:2231–2237.
35. Baker HM, Baker CJ, Smith CA, Baker EN. Metal substitution in transferrins: Specific binding of cerium(IV) revealed by the crystal structure of cerium-substituted human lactoferrin. *J Biol Inorg Chem.* 2000; 5:692–698. [PubMed: 11128996]
36. Park I, et al. Organization of the human transferrin gene: Direct evidence that it originated by gene duplication. *Proc Nat Acad Sci.* 1985; 82:3149–3153. [PubMed: 3858812]
37. He, QY.; Mason, AB. Molecular aspects of release of iron from transferrins. In: Templeton, DM., editor. *Molecular and cellular iron transport.* Marcel Dekker; New York: 2002. p. 95-123.
38. Duffield JR, Taylor DM, Proctor SA. The binding of plutonium to transferrin in the presence of tri-n-butyl phosphate or nitrate and its release by diethylenetriaminepenta-acetate and the tetrameric catechoylamide ligand LICAMC(C). *Int J Nucl Med Biol.* 1986; 12:483–487. [PubMed: 3754852]
39. Durbin PW, Kullgren B, Xu J, Raymond KN. Development of decorporation agents for the actinides. *Radiat Prot Dosimetry.* 1998; 79:433–443.
40. Bali PK, Harris WR. Site-specific rate constants for iron removal from diferric transferrin by nitrilotris(methylenephosphonic acid) and pyrophosphate. *Arch Biochem Biophys.* 1990; 281:251–256. [PubMed: 2168158]

41. Chasteen ND, Williams J. The influence of pH on the equilibrium distribution of iron between the metal-binding sites of human transferrin. *Biochem J.* 1981; 193:717–727. [PubMed: 7305958]
42. Hémadi M, Miquel G, Kahn PH, El Hage Chahine JM. Aluminum exchange between citrate and human serum transferrin and interaction with transferrin receptor 1. *Biochemistry.* 2003; 42:3120–3130. [PubMed: 12627980]
43. Seifert S, Winans RE, Tiede DM, Thiyagarajan P. Design and performance of a ASAXS instrument at the Advanced Photon Source. *J Appl Cryst.* 2000; 33:782–784.
44. Fang X, et al. Mg<sup>2+</sup>-dependent compaction and folding of yeast tRNA<sup>Phe</sup> and the catalytic domain of the *B. subtilis* RNase P RNA determined by small-angle X-ray scattering. *Biochemistry.* 2000; 39:11107–11113. [PubMed: 10998249]
45. Antonio MR, Chiang MH, Seifert S, Tiede DM, Thiyagarajan P. *In situ* measurement of the Preyssler polyoxometallate morphology upon electrochemical reduction. *J Electroanal Chem.* 2008; 626:103–110.
46. Konarev PV, Petoukhov MV, Volkov VV, Svergun DI. Atsas 2.1, a program package for small-angle scattering data analysis. *J Appl Cryst.* 2006; 39:277–286.
47. Cai Z, Lai B, Xiao Y, Xu S. An X-ray diffraction microscope at the Advanced Photon Source. *J Phys IV.* 2003; 104:17–20.
48. McRae R, Lai B, Vogt S, Fahrni CJ. Correlative microXRF and optical immunofluorescence microscopy of adherent cells labeled with ultrasmall gold particles. *J Struct Biol.* 2006; 155:22–29. [PubMed: 16473527]
49. Vogt S. Maps: A set of software tools for analysis and visualization of 3D X-ray fluorescence data sets. *J Phys IV France.* 2003; 104:635–638.

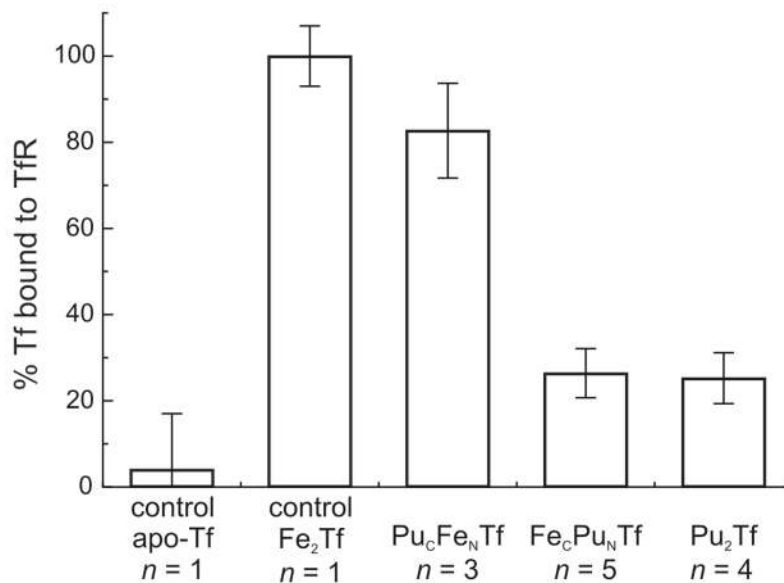


**Figure 1. Pu<sub>C</sub>Fe<sub>N</sub>Tf is the only Pu-transferrin that binds TR well**

Mean binding of 1  $\mu$ M serum transferrin to 1  $\mu$ M soluble TR in 0.2 M NaCl/0.010 M HEPES/0.005 M CO<sub>3</sub><sup>2-</sup> buffered at pH 7.4 as measured by gel chromatography. Error bars are given at the 95% confidence level. For the Pu-transferrins they are  $\pm$ S.E.M. For the control samples, the error bars represent the propagated experimental uncertainties.

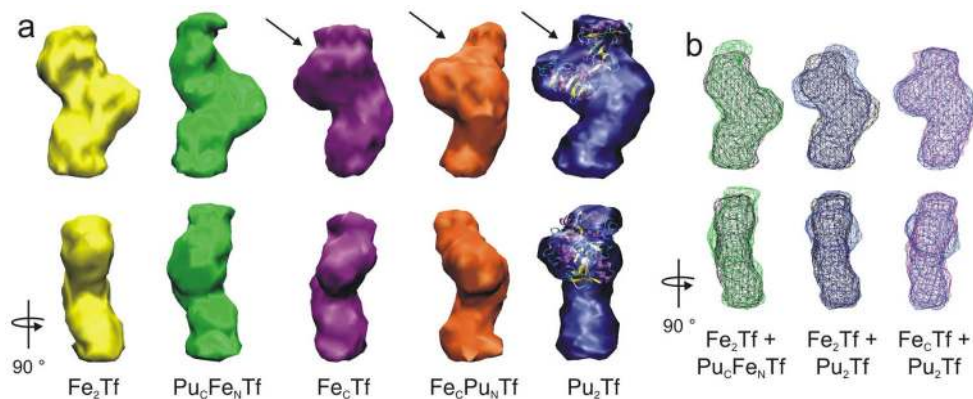


**Figure 2. Structural models of bovine serum transferrins derived from SAXS demonstrate that Pu<sub>C</sub>Fe<sub>N</sub>Tf adopts a closed conformation**

(a) Orthogonal views of the three-dimensional molecular envelopes of metal-transferrin structures reconstructed from the SAXS. The inter-domain cleft in each of the open N-lobes is indicated with arrows, and the open lobe of Pu<sub>2</sub>Tf is superimposed on the crystal structure of open N-terminal recombinant human half apo-transferrin (1BP5)<sup>29</sup>. (b) Docking wireframe representations of the transferrin structures onto each other demonstrates the uniqueness of the closed (Fe<sub>2</sub>Tf and Pu<sub>C</sub>Fe<sub>N</sub>Tf) structures and the mixed (Fe<sub>C</sub>Tf and Pu<sub>2</sub>Tf) structures, with Pu<sub>C</sub>Fe<sub>N</sub>Tf (—), Fe<sub>2</sub>Tf (—), Pu<sub>2</sub>Tf (—), and Fe<sub>C</sub>Tf (—).

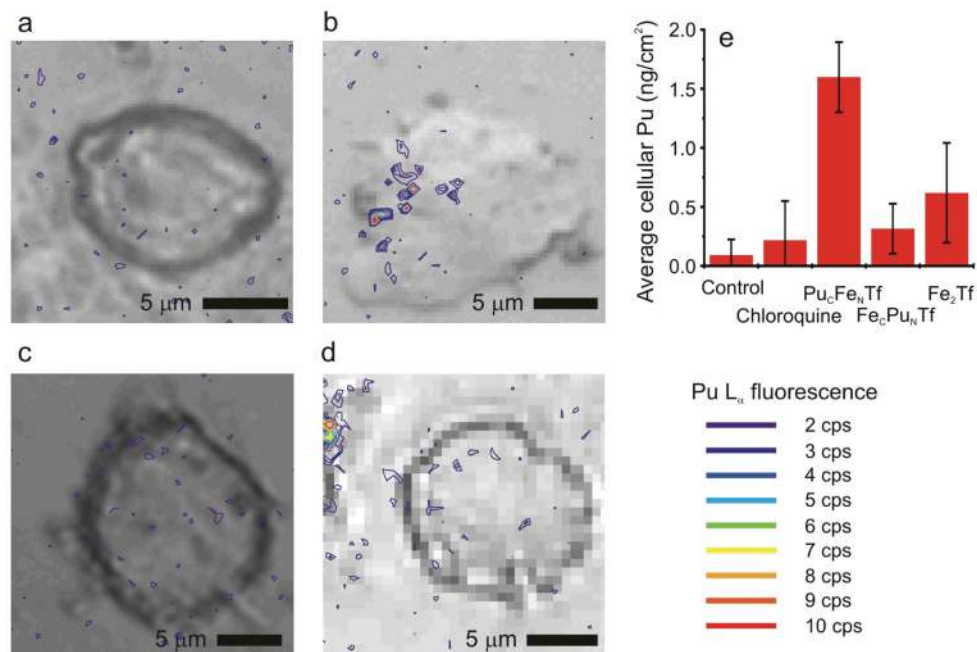


**Figure 3. PC12 cells take in plutonium as Pu<sub>C</sub>Fe<sub>N</sub>Tf**

Contour plots of Pu L $\alpha$  X-ray fluorescence intensity measured by SXFM superimposed on optical images of cells. (a) Pu-free control cell; (b) uptake of Pu as Pu<sub>C</sub>Fe<sub>N</sub>Tf; (c) very low uptake of mixed Fe<sub>C</sub>Pu<sub>N</sub>Tf and of (d) chloroquine-treated cells exposed to Pu<sub>C</sub>Fe<sub>N</sub>Tf. The Pu observed on the left edge of panel d is associated with cellular debris. The average background corrected Pu content (e) of the Pu-containing cells exposed to closed Pu<sub>C</sub>Fe<sub>N</sub>Tf (labeled “Pu<sub>C</sub>Fe<sub>N</sub>Tf”,  $n = 8$ ) is greater than that of control cells (labeled “Control”,  $n = 20$ ), cells simultaneously treated with 50  $\mu$ M chloroquine and Pu<sub>C</sub>Fe<sub>N</sub>Tf (labeled “Chloroquine”,  $n = 8$ ), cells exposed to Fe<sub>C</sub>Pu<sub>N</sub>Tf (labeled “Fe<sub>C</sub>Pu<sub>N</sub>Tf”,  $n = 21$ ), or cells exposed to an equimolar mixture of Fe<sub>2</sub>Tf and Pu<sub>C</sub>Fe<sub>N</sub>Tf (labeled “Fe<sub>2</sub>Tf”,  $n = 4$ ). The error bars are  $\pm$ S.E.M. at 95% confidence.